



# Zinc-blende GaN quantum dots grown by vapor–liquid–solid condensation

T. Schupp<sup>a,\*</sup>, T. Meisch<sup>b</sup>, B. Neuschl<sup>b</sup>, M. Feneberg<sup>b</sup>, K. Thonke<sup>b</sup>, K. Lischka<sup>a</sup>, D.J. As<sup>b</sup>

<sup>a</sup> Universität Paderborn, Department Physik, Warburger Str. 100, 33095 Paderborn, Germany

<sup>b</sup> Institut für Quantenmaterie/Gruppe Halbleiterphysik, Universität Ulm, 89069 Ulm, Germany

## ARTICLE INFO

Available online 21 December 2010

### Keywords:

A1. Atomic force microscopy  
 A1. Growth models  
 A1. Nanostructures  
 A1. Reflection high energy electron diffraction  
 A3. Molecular beam epitaxy  
 B1. Nitrides

## ABSTRACT

Vapor–liquid–solid condensation was utilized to fabricate zinc-blende GaN quantum dots on 3C-AlN (0 0 1) in a molecular beam epitaxy system. By adjustment of deposition parameters and nitridation procedure the density of the quantum dots was controllable in the range of  $5 \times 10^8$ – $5 \times 10^{12}$  cm<sup>-2</sup>. The quantum dots in the range of  $8 \times 10^{10}$ – $5 \times 10^{12}$  cm<sup>-2</sup> have shown strong optical activity in photoluminescence spectroscopy. Furthermore we have demonstrated that vapor–liquid–solid condensation is suitable to tune the emission energy of zinc-blende GaN quantum dots in the range of 3.55–3.81 eV.

© 2011 Elsevier B.V. All rights reserved.

## 1. Introduction

In recent years a growing interest in wide-bandgap quantum dots (QDs) based on group-III nitrides is observed. With the ongoing commercial success of nitride based light emitting diodes, the realization of optical and quantum optical devices based on nitride QDs seems to be the next logical step. Wurtzite GaN based single quantum dots were successfully utilized as single-photon emitters showing photon antibunching and triggered single-photon generation [1]. However, the quantum confined Stark effect, caused by “built-in” electric fields, leads to reduced recombination probability of electrons and holes in confined states and therefore low repetition rate photonic devices. In contrast, the metastable zinc-blende (cubic) phase of AlN (c-AlN) and GaN (c-GaN) has no polarization fields in the (0 0 1) growth direction [2]. Consequently, the radiative recombination time of c-GaN QDs was measured to be two orders of magnitude below the recombination time of wurtzite GaN QDs [3].

Until recently the only method to fabricate self-organized c-GaN QDs was Stranski–Krastanov (SK) growth [4]. We show an alternative growth method of c-GaN quantum dots by droplet epitaxy, a vapor–liquid–solid (VLS) process. In droplet epitaxy a defined amount of Ga is deposited on the substrate surface, forms droplets and is then nitridated by a N plasma. The size and distance between the Ga droplets can be controlled by a combination of amount of deposited Ga, substrate temperature and time before nitridation [5]. In contrast to the SK growth method, droplet epitaxy can create QDs of not only high density but also low density, covering the range from  $5 \times 10^8$  to  $5 \times 10^{12}$  cm<sup>-2</sup>. In this contribution, we report on the

droplet epitaxy of c-GaN QDs with distinct size control to tune the QD emission energy in the range of 3.55–3.81 eV.

## 2. Experimental procedure

The c-GaN QDs and the c-AlN buffer were grown in a Riber 32 MBE system including an Oxford Instruments N plasma cell and standard Ga and Al effusion cells. In-situ growth monitoring was achieved by reflection high energy electron diffraction (RHEED). The surface structure of the samples was analyzed by atomic force microscopy (AFM). To obtain optical data, photoluminescence (PL) spectroscopy was carried out. The samples were excited by an ArF excimer laser with  $\lambda = 193$  nm. PL was detected by a liquid nitrogen cooled charge coupled device camera mounted to a grating monochromator with a focal length of  $f = 1$  m.

## 3. Results and discussion

At first the 3C-SiC (0 0 1) substrate is cleaned by an Al deposition and desorption process, followed by the growth of a 30 nm thick c-AlN (0 0 1) barrier layer at 730 °C substrate temperature [6]. The RHEED pattern of the AlN surface in Fig. 1(a) shows long thin streaks, indicating a smooth two-dimensional surface [7].

Fabrication of the c-GaN QDs begins with the deposition of a defined amount of Ga, equivalent to 1–12 ML. The strong cohesion force between the Ga atoms induces the formation of droplets. The distance between the Ga droplets is influenced by the amount of deposited Ga and the surface diffusion length, controlled by the substrate temperature [5]. For this sample series an AlN surface temperature of 350 °C was used.

\* Corresponding author. Tel.: +49 5251 60 5831; fax: +49 5251 60 5843.  
 E-mail address: [schupp@post.com](mailto:schupp@post.com) (T. Schupp).

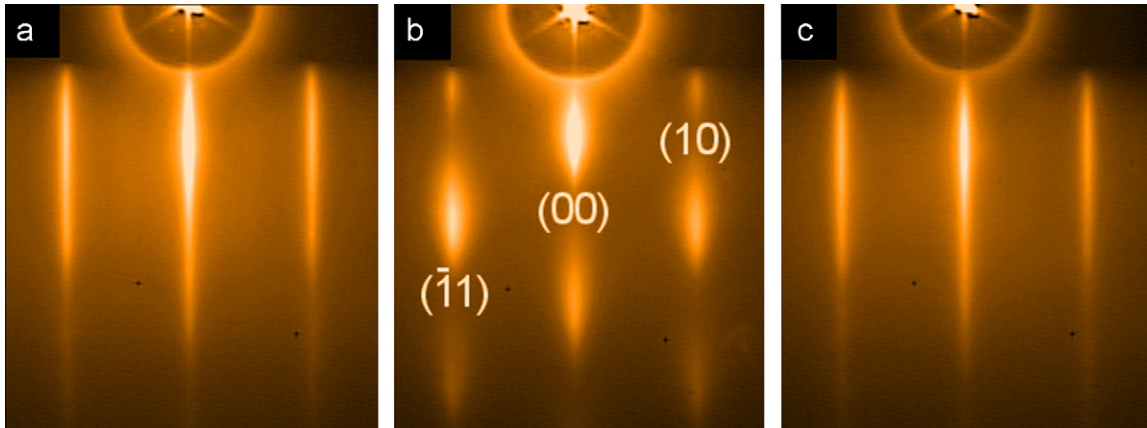


**Fig. 1.** RHEED patterns: (a) reflections of the c-AlN layer—long thin streaks indicate a smooth 2D surface, (b) reflections of c-GaN droplet QDs—the spotty reflections indicate 3D islands of cubic crystal structure and (c) reflections of c-AlN after 30 ML QD overgrowth—long thin streaks indicate a smooth 2D surface.

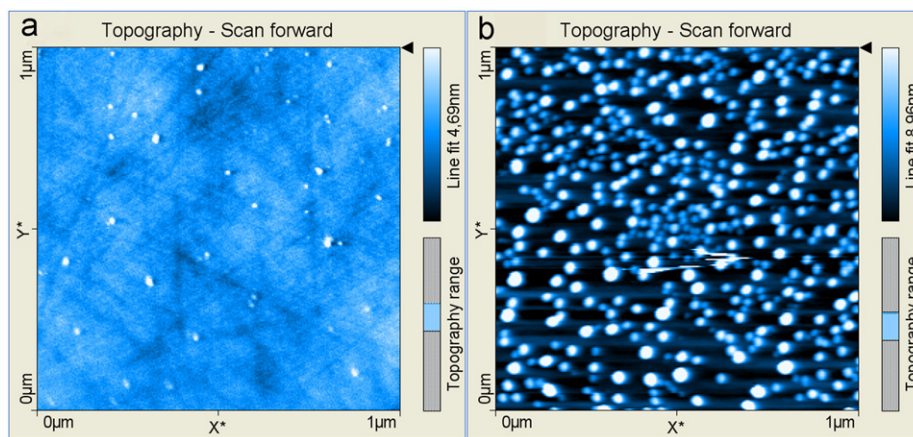


**Fig. 2.** AFM images: (a)  $1 \times 1 \mu\text{m}^2$  GaN QDs grown by method A on c-AlN, the average width of the QDs is 10 nm, the height 2.5 nm and the density  $5 \times 10^9 \text{ cm}^{-2}$  and (b)  $1 \times 1 \mu\text{m}^2$  GaN QDs grown by method B on c-AlN, the average width of the QDs is 20 nm, the height 3 nm and the density  $9 \times 10^{10} \text{ cm}^{-2}$ .

In the next step the Ga droplets are nitrated by exposure to the N plasma beam for 3–15 min. Depending on the desired QD density two different nitridation methods can be applied. In method A the substrate temperature stays constant during the nitridation step and is increased to 730 °C afterwards. In method B the substrate temperature is ramped up to 730 °C during the nitridation. The RHEED patterns for both methods show a strong increase in intensity and the appearance of spotty reflections, as demonstrated exemplarily in Fig. 1(b). Resulting from an electron transmission component through three dimensional islands, the spotty reflections are an indication of quantum dots on the surface [7]. Selective area electron diffraction, a method of transmission electron microscopy, illustrates the relation between GaN reciprocal space reflections of zinc-blende and hexagonal phase [8]. This relation of the reflection positions can also be observed in RHEED. Especially two reflections of the hexagonal GaN phase can be observed in RHEED on the diagonal of the zinc-blende GaN (0 0) reflection to the (1 0) reflection, if a hexagonal contribution is present. As all reflections in the RHEED pattern can be attributed to the zinc-blende lattice structure, cubic phase purity can be concluded within detection limits [8]. The sensitivity limit for the detection of reflections of the hexagonal GaN phase is 2% content, determined by thick c-GaN layers with varying hexagonal GaN phase content measured in RHEED and by high resolution X-ray diffraction [9]. The c-GaN QDs are overgrown by a 30 nm c-AlN barrier layer at 730 °C substrate temperature. The RHEED pattern in Fig. 1(c) of the

AlN surface after QD overgrowth shows long thin streaks and absence of spotty reflections. Consequently, a smooth surface with full epitaxial overgrowth of the GaN QDs can be concluded. AFM measurements of the AlN surface after GaN QD overgrowth, not shown here, confirm a smooth surface.

The size and density of the QDs are measured by AFM of uncapped GaN QDs. Two aspects are of interest: the deposited Ga amount and the nitridation method. A series of samples with varying Ga amount, grown by method B, was analyzed by AFM. The correlation found was an increase in QD size and density on increasing the amount of supplied Ga. The second, more surprising, aspect is the strong influence of the nitridation method. The AFM image in Fig. 2(a) shows a  $1 \times 1 \mu\text{m}^2$  area of the AlN surface covered with GaN QDs grown by method A. The average width of the QDs is 10 nm, the average height 2.5 nm and the density is  $5 \times 10^9 \text{ cm}^{-2}$ . Fig. 2(b) shows an AFM image of a  $1 \times 1 \mu\text{m}^2$  area of the AlN surface covered with GaN QDs with an equal amount of supplied Ga, but grown by method B. Counting the QDs, a density of  $9 \times 10^{10} \text{ cm}^{-2}$ , an average width of 20 nm and a height of 3 nm can be determined. In comparison, given an equal amount of deposited Ga, nitridation method B yields bigger QDs of higher density. The phase equilibrium of liquid Ga and solid GaN inside the droplet could be the origin of the observed difference [10] as further GaN condensation requires supersaturation of Ga and limits the GaN growth at the given temperature. Furthermore, additional GaN growth occurs during the desorption of excess Ga at higher temperatures.

In comparison, the main difference between both methods is the lack of additional N supply in method A during the heat-up and Ga desorption process. The N solubility in Ga is lower than 1%, so only a small amount of N is available in the droplets to form GaN [10]. A second effect occurs during the heating process, namely Ostwald ripening, which causes the coalescence of neighboring QDs, leading to larger but more distant QDs [11]. In contrast, method B supplies additional N during the heating and Ga desorption process. This additional N influences the GaN QD formation in two ways. Firstly, more N simply leads to the growth of more GaN compared to method A. Secondly, the nitrogen termination of the surface increases the surface diffusion barrier for Ga and decreases the diffusion length of the Ga adatoms [12]. This leads to trapping of the Ga inside the droplets until nitridation and reduces Ostwald ripening. Consequently, the density of the GaN QDs fabricated with method B is higher.

For this reason designing size and density of QDs by droplet epitaxy is a two-step process with the first step being selection of the nitridation method to define the order of magnitude of the density of QDs and the second step being adjustment of the deposited Ga amount to fine-tune the size and density of the QDs.

The photoluminescence spectrum of a single QD has a very narrow full width at half maximum (FWHM), compared to the broad emission band of the bulk material. Thus, the single QD emission can be idealized as a delta peak. The superposition of all the QDs emission delta peaks forms the emission band of a given sample as a whole. The ensemble of QDs excited by the ArF laser is in the order of  $10^8$  QDs; consequently the shape of the emission is correlated to the size distribution of the QDs. Additionally, earlier research on SK c-GaN QDs has shown that the determining factor for the QD emission energy is the height of the QD [13]. To analyze these aspects for droplet epitaxy grown c-GaN QDs, comparable samples with and without 30 nm AlN cap layer have been grown with method B, as capped QDs cannot be measured by AFM and uncapped QDs did not show PL. The PL spectrum of a typical c-GaN QD sample at 10 K can be seen in Fig. 3. A Gaussian shaped emission band with an intensity maximum at an energy of  $3.625 \pm 0.01$  eV can be identified. Moreover, a high energy tail indicates skewed size distribution towards smaller QDs. The average height of the uncapped QDs has been measured by AFM to be  $3.1 \pm 0.1$  nm. For a QD height of 3.1 nm above the wetting layer, theoretical work of Fonoberov and Balandin [13] on c-GaN SK QDs predicts an exciton

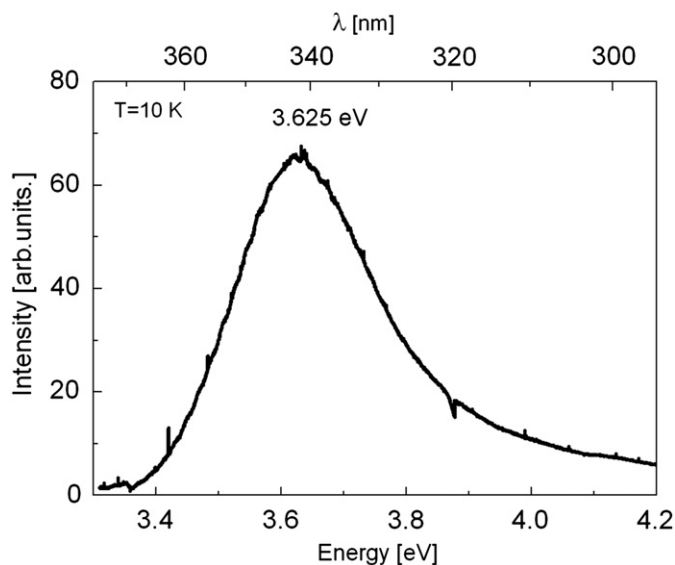


Fig. 3. Photoluminescence spectrum of c-GaN droplet QDs. A Gaussian shaped emission band was identified, its central energy being at  $3.61 \pm 0.01$  eV.

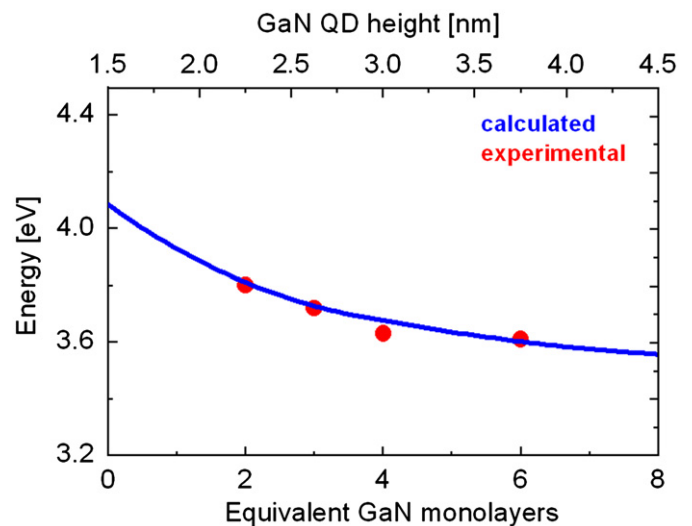


Fig. 4. Relations between deposited Ga amount, QD height and QD emission energy. The dots mark the measured QD emission energies of 4 samples. The graph shows the calculated QD emission energy over QD height relation.

ground state transition energy of 3.62 eV. The measured energy is in good agreement with the calculated energy for c-GaN SK QDs, if we take into account the deviation of the AFM measurement, the potentially different shape of the droplet QDs and the likely lack of a wetting layer. Transmission electron microscopy would have been suitable to investigate this in more detail, but was not available. The PL spectra of QDs samples with a deposited Ga amount of 2, 3, 4 and 6 ML show a decrease in emission energy from 3.81 to 3.55 eV with increasing Ga deposition, as shown by the dots in Fig. 4. Comparing the deposited Ga amount with the AFM measured QD height bares a linear relation in the region of 2–6 ML. Accordingly, the relation between QD height and emission energy can be followed. This relation can be seen in Fig. 4, as the measured dots are in good agreement with the calculated curve of dependence of QD height on QD emission energy [13]. As a result, the emission energy of a QD sample can be varied depending on the deposited Ga amount.

#### 4. Conclusion

In summary, we have demonstrated that vapor–liquid–solid condensation is suitable to fabricate optically active zinc-blende GaN QDs. The density of the quantum dots was controllable in the range of  $5 \times 10^8$ – $5 \times 10^{12}$   $\text{cm}^{-2}$  by adjustment of deposition parameters and nitridation procedure. However, only high density quantum dots in the range of  $8 \times 10^{10}$ – $5 \times 10^{12}$   $\text{cm}^{-2}$  have shown strong photoluminescence. Finally, it was shown that droplet epitaxy can be utilized to tune the emission energy of zinc-blende GaN quantum dots in the range of 3.55–3.81 eV by the variation of the deposited Ga amount.

#### Acknowledgements

This work was supported by the DFG Graduate Program GRK 1464 “Micro- and nanostructures in optoelectronics and photonics”. We would like to thank Dr. M. Abe and Dr. H. Nagasawa of HOYA Corporation for supplying the 3C-SiC substrates.

#### References

- [1] C. Santori, S. Götzinger, Y. Yamamoto, S. Kako, K. Hushino, Y. Arakawa, Appl. Phys. Lett. 87 (2005) 051916.
- [2] D.J. As, Microelectron. J. 40 (2009) 204.

- [3] J. Simon, N.T. Pelekanos, C. Adelman, E. Martinez-Guerrero, R. André, B. Daudin, Le Si Dang, H. Mariette, Phys. Rev. B 68 (2003) 035312.
- [4] E. Martinez-Guerrero, F. Chabuel, B. Daudin, J.L. Rouviere, H. Mariette, Appl. Phys. Lett. 81 (2002) 5117.
- [5] N. Koguchi, Mater. Res. Soc. Symp. Proc 959 (2007) 18.
- [6] T. Schupp, K. Lischka, D.J. As, J. Cryst. Growth 312 (2010) 1500.
- [7] W. Braun, Applied RHEED, Springer Tracts in Modern Physics, vol. 154, Springer, Berlin, 1999.
- [8] S. Sanorpim, E. Takuma, H. Ichinose, R. Katayama, K. Onabe, Phys. Status Solidi B 244 (1769) 2007.
- [9] Y. Suzuki, M. Shinbara, H. Kii, Y. Chikaura, J. Appl. Phys. 101 (2007) 063516.
- [10] A.V. Davydov, W.J. Boettinger, U.R. Kattner, T.J. Anderson, Phys. Status Solidi A 188 (2001) 407.
- [11] R.D. Vengrenovich, Semiconductors 35 (2001) 1378.
- [12] T. Zywiets, J. Neugebauer, M. Scheffler, Appl. Phys. Lett. 73 (1998) 487.
- [13] V.A. Fonoberov, A.A. Balandin, J. Appl. Phys. 94 (2003) 7178.